

2021

EIC Crab Cavity Multipole Analysis

Q. Wu

Y. Luo

B. Xiao

Subashini De Silva

Old Dominion University, pdesilva@odu.edu

J. A. Mitchell

Follow this and additional works at: https://digitalcommons.odu.edu/physics_fac_pubs



Part of the [Engineering Physics Commons](#)

Original Publication Citation

Wu, Q., Luo, Y., Xiao, B. P., De Silva, S. U., & Mitchell, J. A. (2021) EIC crab cavity multipole analysis. In L. Lin, J.M. Byrd, R. Neuenschwander, & V.R.W. Schaa (Eds.), *Proceedings of the 12th International Particle Accelerator Conference* (pp. 2589-2591) Joint Accelerator Conferences Website. <https://doi.org/10.18429/JACoW-IPAC2021-WEPAB006>

This Conference Paper is brought to you for free and open access by the Physics at ODU Digital Commons. It has been accepted for inclusion in Physics Faculty Publications by an authorized administrator of ODU Digital Commons. For more information, please contact digitalcommons@odu.edu.

MULTIPOLE CALCULATION AND CONVERGENCE STUDY

A vacuum volume model of the RF Dipole crab cavity design at 197 MHz for EIC is shown in Fig. 2. This model is used for the multipole convergence study and preliminary dynamic aperture tracking. The EM field for this design is shown in Fig. 3.

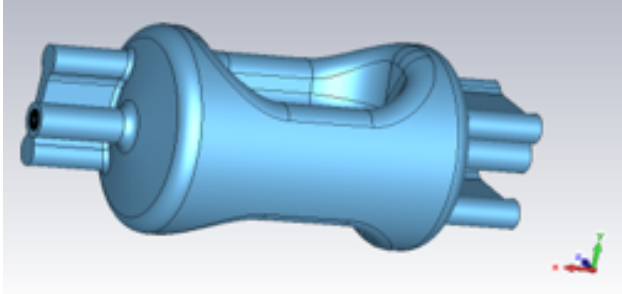


Figure 2: Vacuum volume of the EIC crab cavity.

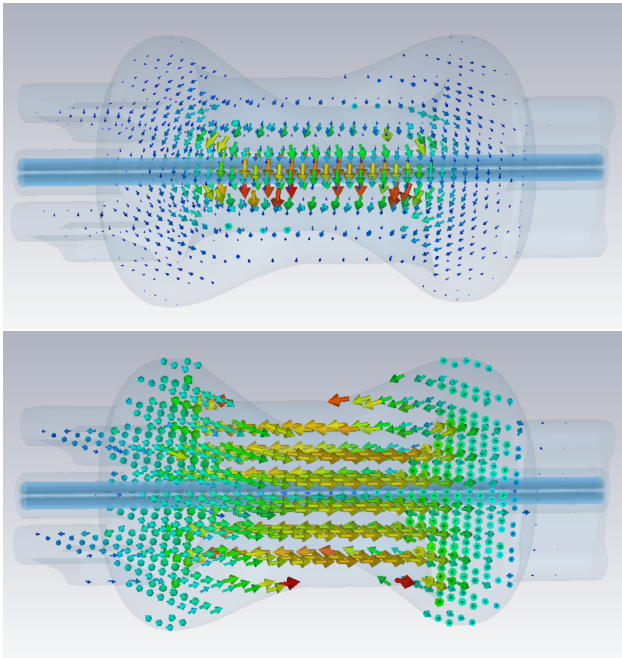


Figure 3: Electric (top) and Magnetic (bottom) field of the crab cavity.

The EM field at a specified radius r along the beam axis is extracted from the CST simulations, and then integrated in a Python code to calculate for the multipole strength at each order. The normal multipole strength b_n along the beam axis is calculated by local integration as shown in Fig. 4.

Two methods were used to calculate the multipoles: Using only the longitudinal electric field at radius r with Panofsky–Wenzel Theorem (PW), and using both transverse electric and magnetic field at the same radius to calculate the Lorentz Force (LF). The two methods converge differently with the mesh size and the radius r . Based on the symmetry of the model and the horizontal placement configuration,

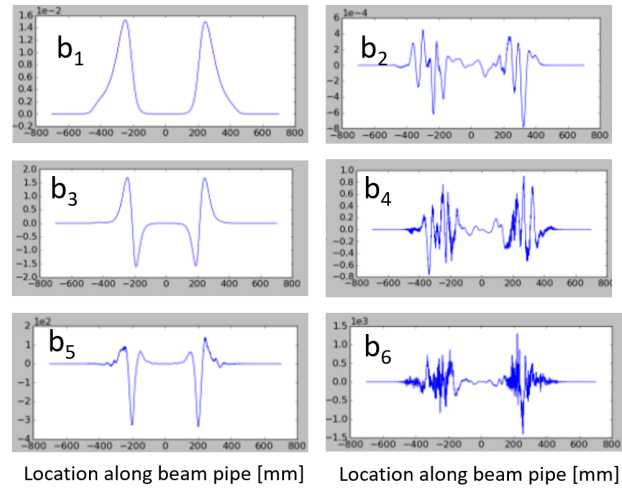


Figure 4: Normal multipole strength b_n along beam axis. The vertical axis of each plot has the unit of $\text{mTm}/\text{m}^{n-1}$.

all skew multipole strength a_n should be negligible, compared to the normal multipole strength b_n . In addition, the quadrupolar component b_2 , b_4 , and b_6 are zero in the case of perfect symmetry. However, it is worth to notice that due to fabrication errors and ancillary components, these values should deviate from zero during operation. The tolerance of the fabrication and alignment errors should be defined with dynamic aperture tracking with crab cavity multipoles.

Higher order multipoles are harder to converge due to signal to systematic noise ratio in simulation (same problem in actual measurement), therefore the value of b_4 and b_6 are used in the multipole calculation to determine the parameters in EM field simulation for the cavity, as well as compare the two methods used for calculation. Figures 5 and 6 shows the comparison of PW and LF methods with different mesh size and radius r respectively. In both comparisons, LF method gives relatively closer to zero b_4 and b_6 with acceptable mesh size and radius.

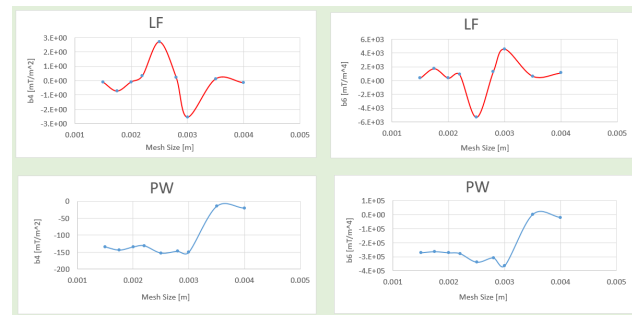


Figure 5: Comparison of PW and LF methods with respect to the mesh size in EM field simulation.

The b_n and a_n values used for dynamic aperture tracking are listed in Table 1, with 2 mm mesh size in both transverse and longitudinal directions in EM simulation and extracting the field at the radius of 20 mm.

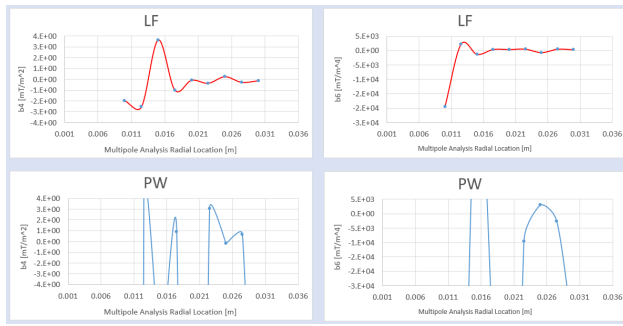


Figure 6: Comparison of PW and LF methods with respect to the specified field extraction radius in EM field simulation.

Table 1: Multipole Strength

n	b_n [mTm/m ⁿ⁻¹]
1	2.810×10^1
2	3.542×10^{-5}
3	4.412×10^2
4	-8.561×10^{-2}
5	-2.199×10^4
6	3.513×10^2

Dynamic Aperture Tracking

The dynamic aperture tracking included all components in the interaction region with errors on the magnets. Preliminary radial dynamic aperture tracking results are shown in Fig. 7.

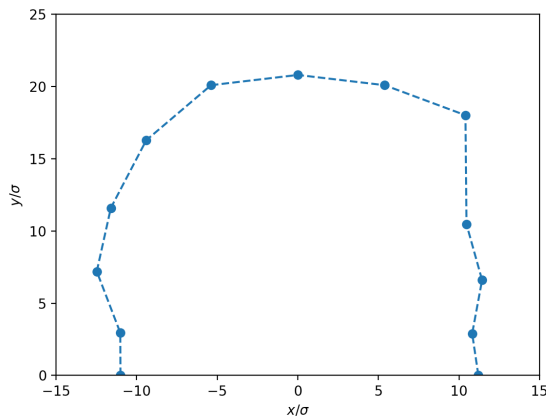


Figure 7: Preliminary tracking results of the DA tracking with crab cavities.

The dynamic aperture in Fig. 7 is defined as $N = \sqrt{N_x^2 + N_y^2}$, where N_x and N_y are the two orthogonal phase space for DA searching in the unit of rms beam size in x and y directions.

The tracking assumed a total operation voltage of 25.82 MV from each 197 MHz crab cavity set, and the 394 MHz cavities are not included here. The simulation also assumed all crab cavity multipoles located at the center

of the cavity chain at the installation site. The skew multipole strength a_n is multi-orders of magnitude smaller compare to the strength of the normal multipoles, with the assumption of ideal cavities and precise alignment during installation. Therefore, these result shown in Fig. 7 neglected the affect from the skew multipoles.

CONCLUSION

In the current design, the EIC will install two sets of crab cavities on each side of the detector symmetrically to implement local crabbing. These cavities are not axial symmetric and therefore the excited higher order multipoles may provide some limitation to the dynamic aperture in the interaction region. The analysis of these multipoles provided guidance for parameters during EM field simulations with limited computing resources. The preliminary tracking results show that the dynamic aperture with crab cavities is 11 sigma of the radial beam size.

The next steps for multipole calculation would be include RF couplers and empirical fabrication error to the cavity EM field, as well as allow some tolerance for the installation of these cavities in the tunnel.

ACKNOWLEDGEMENT

The authors would like to thank Kai Papke for sharing the Macro for extracting the EM field from the CST Studio.

REFERENCES

- [1] C. Montag *et al.*, “Design Status Update of the Electron-Ion Collider”, presented at the 12th Int. Particle Accelerator Conf. (IPAC’21), Campinas, Brazil, May 2021, paper WEPAB005, this conference.
- [2] H. Witte *et al.*, “The Interaction Region of the Electron-Ion Collider”, presented at the 12th Int. Particle Accelerator Conf. (IPAC’21), Campinas, Brazil, May 2021, paper WEPAB002, this conference.
- [3] J. B. García *et al.*, “Long Term Dynamics of the High Luminosity Large Hadron Collider with Crab Cavities”, *Phys. Rev. Accel. Beams*, vol. 19, p. 101003, 2016. doi:10.1103/physrevaccelbeams.19.101003
- [4] S. De Silva *et al.*, “Design of an RF-Dipole Crabbing Cavity System for the Electron-Ion Collider”, presented at the 12th Int. Particle Accelerator Conf. (IPAC’21), Campinas, Brazil, May 2021, paper MOPAB393, this conference.
- [5] CST Microwave Studio Suite 2020, <https://www.3ds.com/products-services/simulia/products/cst-studio-suite/>.
- [6] J. A. Mitchell, “Higher Order Modes and Dampers for the LHC Double Quarter Wave Crab Cavity”, Ph.D. thesis, Lancaster University, Lancaster, United Kingdom, 2019.
- [7] Y. Luo, “SimTrack: A compact c++ code for particle orbit and spin tracking in accelerators”, *Nucl. Instrum. and Methods A*, vol. 801, pp. 95-103, 2015. doi:10.1016/j.nima.2015.08.014